Nanotechnology

PAPER

Atomic layer etching of chrome using ion beams

To cite this article: Jin Woo Park *et al* 2019 *Nanotechnology* **30** 085303

View the article online for updates and enhancements.

IOP ebooks™

Bringing you innovative digital publishing with leading voices to create your essential collection of books in STEM research.

Start exploring the collection - download the first chapter of every title for free.

This content was downloaded from IP address 115.145.196.110 on 31/12/2018 at 01:18

Nanotechnology 30 (2019) 085303 (8pp) https://doi.org/10.1088/1361-6528/aaf521

Atomic layer etching of chrome using ion beams

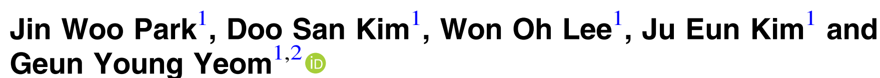
Jin Woo Park[1], Doo San Kim[1], Won Oh Lee[1], Ju Eun Kim[1] and Geun Young Yeom[1,2]

[1] School of Advanced Materials Science and Engineering, Sungkyunkwan University, Suwon 16419, Republic of Korea
[2] SKKU Advanced Institute of Nano Technology (SAINT), Sungkyunkwan University, Suwon 16419, Republic of Korea

E-mail: gyyeom@skku.edu

Received 20 August 2018, revised 22 November 2018
Accepted for publication 30 November 2018
Published 28 December 2018

Abstract

In this study, two Cr atomic layer etching (ALE) methods have been applied for the precise control of Cr etching. The first one involves O radical adsorption followed by Cl^+ ion desorption (ALE with chemical ion desorption; chemical anisotropic ALE), and the second one involves Cl/O radical adsorption followed by Ar^+ ion desorption (ALE with physical ion desorption; physical anisotropic ALE). Their effects on Cr etch characteristics were also investigated. For both the ALE methods, saturated Cr etch depth/cycle of 1.1 and 1.5 Å/cycle were obtained for the chemical and physical anisotropic ALE, respectively, while maintaining near-infinite etch selectivities with various Si-based materials like silicon, silicon dioxide, and silicon nitride. The Cr etch depth could be controlled precisely with atomic precision by controlling the etch cycles for both Cr ALE methods in addition to the infinite etch selectivities over Si-based materials. Further, the original surface roughness and chemical composition of Cr surface were maintained after Cr ALE. The ALE technique can be used to precisely control the thickness of materials, including metals such as Cr, without any surface damage.

Supplementary material for this article is available online

Keywords: atomic layer etching, chrome, ion beam, adsorption, desorption, x-ray photoelectron spectroscopy

(Some figures may appear in colour only in the online journal)

1. Introduction

Atomic layer etching (ALE) can be applied to sophisticated processes requiring atomic-level precision similar to atomic layer deposition in semiconductor manufacturing, and is attracting particular attention as a technology for next-generation nanoscale semiconductor fabrication [1–6]. These atomic precision techniques have been investigated for various materials such as silicon, III–V compounds, dielectrics, and even two-dimensional materials for more than 20 years [7–14]. Currently, in the semiconductor industry, ALE techniques are applied to highly selective self-aligned contact etch for logic devices and precise etch control with low-etch damage for nanoscale etching [11, 12]. Further, as the device size is decreased, ALE techniques can be applied more frequently in semiconductor device fabrication.

In semiconductor device fabrication, a photomask is used to transfer electronic circuits onto a substrate. The uniformity of the critical dimension (CD) of the photomask is important for nanoscale high-intergraded circuits for the fabrication of next-generation semiconductor devices [15, 16]. The photomask generally consists of quartz, chrome (Cr), and molybdenum silicide (MoSi). Depending on the type of photomask such as standard chrome on glass, opaque MoSi on glass, and phase-shifting mask, Cr is dry etched and used as a hard mask to fabricate the photomask owing to the low-etch selectivity between MoSi and quartz [17–19]. Thus, the dry etch process of Cr with a low surface

 © 2018 IOP Publishing Ltd Printed in the UK

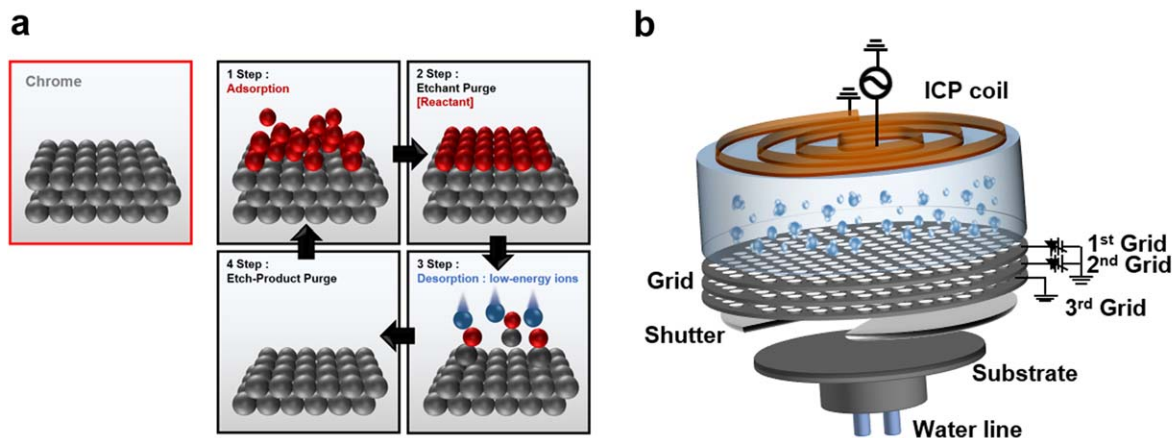

Figure 1. (a) Concept of Cr ALE cycles. (b) Schematic diagram of ICP ion beam source with three-grid assembly used to etch Cr by ALE.

damage and high-uniformity is important in determining the CD of the photomask.

In the conventional dry etching of Cr using conventional inductively coupled plasma-reactive ion etching (ICP-RIE), the CD uniformity is reduced owing to the plasma non-uniformity, and the photomask surface can be damaged easily at high-bias power conditions [20–23]. It is believed that ALE is an etching technique that can achieve low-damage, high-etch selectivity, and high-etch uniformity regardless of plasma uniformity, thus enabling the fabrication of a high-resolution photomask by etching the materials constituting the photomask such as Cr, MoSi, and quartz for lithographic patterning. Therefore, to overcome these drawbacks in ICP-RIE, the possibility of etching Cr precisely in the atomic scale using ALE techniques is investigated in this study.

The ALE is a cyclic etch process and consists of adsorption and desorption steps. In the adsorption step, reactive radicals are adsorbed chemically on the material surface to form a chemisorbed layer on the surface; in the desorption step, the chemisorbed layer formed on the surface is desorbed from the surface by low-energy ion bombardment. In this study, the possibility of Cr ALE has been investigated by two methods using O or Cl/O radicals for adsorption and low-energy Cl^+ or Ar^+ ion beam for desorption during the etch cycle for the precise control of etch depth and to minimize the surface damages of Cr. Furthermore, the etch mechanisms of both Cr ALE methods were investigated. For both Cr ALE methods, the controlled Cr etch depth per cycle and extremely high-etch selectivity of Cr over various Si-based materials like silicon, silicon dioxide, and silicon nitride could be achieved in addition to minimized surface damage.

2. Experimental

The sample used for Cr ALE is a 100 nm thick Cr thin film on SiO_2 wafers deposited by an e-beam evaporator. To measure the Cr etch depth/cycle during the ALE, the samples patterned with photoresist (PR) were etched for 100 cycles, and the total etch depths were estimated after the removal of the PR. The total etch depths were determined by a surface profilometer (Tencor Instrument, Alpha step 500). The measured etch depth was divided by the total number of ALE cycles to yield the etch depth/cycle. To investigate the etch selectivities of Cr over other silicon-based materials like Si, SiO_2, and Si_3N_4, these materials deposited on silicon wafers were also prepared and etched together during the ALE of Cr. The changes in Cr surface roughness after ALE were measured using atomic force microscopy (AFM; Bruker Innova). Furthermore, the surface composition of Cr after ALE was analyzed by x-ray photoelectron spectroscopy (XPS; Thermo VG, MultiLab 2000, Mg $K\alpha$ source). To compare the compositions of Cr surfaces etched by ALE and the conventional RIE, Cr samples were also etched using an ICP-RIE etcher operated at 13.56 MHz, 100 W source power and 13.56 MHz, 50 W bias power for 5 min with 5.0 mTorr of Cl_2 and Cl_2/O_2 (1:1).

Figures 1(a) and (b) show the concept of the Cr ALE cycle and the ICP ion beam source with a three-grid assembly used to etch Cr by ALE, respectively. As shown in figure 1(a), one ALE cycle is composed of four sequential steps; the first step (adsorption step) is for the adsorption (chemisorption) of reactant species on the surface, and the third step (desorption step) is for the desorption (removal) of the surface chemisorbed species on the surface. The second and fourth steps are for purging residual reactant species and desorbed chemisorbed species from the surface, respectively. As shown in figure 1(b), a three-grid (graphite grid, hole size is 2 mm in diameter, and the open ratio is 43%) ICP-type ion source operated at a 13.56 MHz radio-frequency (RF) was used for the formation of radicals (during the adsorption step) and low-energy ions (during the desorption step). In this grid assembly, a positive voltage was applied to the first grid located close to the source (acceleration grid) for ion energy control, and a negative voltage was applied to the second grid for ion beam flux control and electron shielding. Further, the third grid was grounded. The base pressure of the ALE chamber is approximately 2.0×10^{-5} Torr.

Two different Cr ALE methods, i.e. (case I) a chemical anisotropic ALE method, and (case II) a physical anisotropic ALE method, were investigated. Figure 2 shows the process

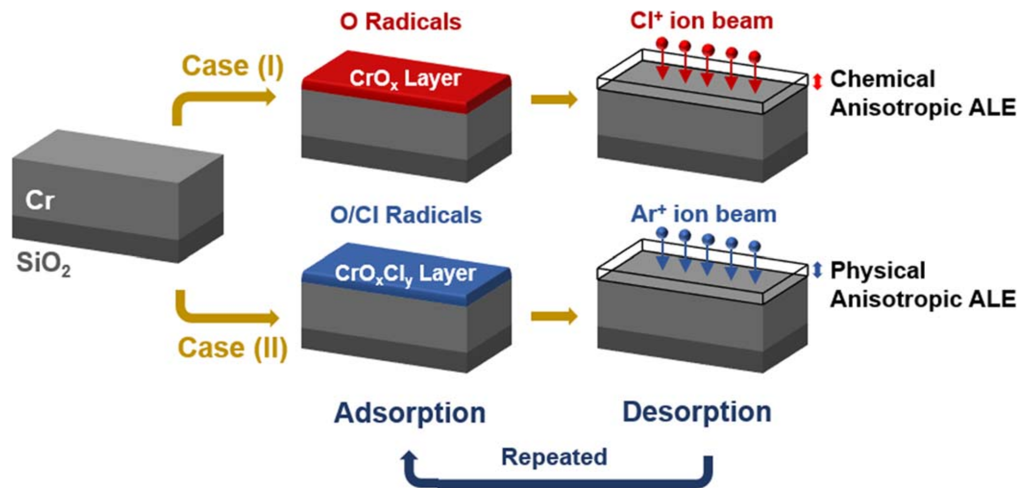

Figure 2. Process steps of two Cr ALE methods: (I) chemical anisotropic ALE method, and (II) physical anisotropic ALE methods.

steps of two different Cr ALE methods. For the all ALE conditions, 300 W of RF power was applied to the ICP source for both the adsorption step and desorption step while maintaining the process chamber pressure at ∼2.0 mTorr. (I) For the chemical anisotropic ALE method, during the adsorption step, 50 sccm of O_2 gas was used without applying any voltage to the grids for oxygen radical generation and to chemisorb oxygen radicals on the Cr surface [24, 25]. For the desorption step, 50 sccm of Cl_2 gas was used while applying +10 to +70 V to the first grid, and fixed at −100 V to the second grid for the extraction of directional Cl^+ ion beams and to desorb the chemisorbed species (Cl radicals are also generated during Cl^+ ion formation for the desorption step; however, the effect on ALE was not significant for the optimized condition of +10 V for the exposure time/cycle of less than 20 s/cycle. Therefore, the effect of radicals on ALE was ignored). (II) For the physical anisotropic ALE method, during the adsorption step, 50 sccm/50 sccm of Cl_2/O_2 (1:1) gas was used without applying any voltage to the grids for the generation of Cl/O radicals and to chemisorb oxychlorides on the Cr surface [24, 25]. (During the generation of Cl/O radicals for the adsorption step, low-energy ions can be extracted by the plasma potential from the ion beam source, and they can bombard the surface in addition to radicals during the adsorption. It could etch the material surface during the adsorption step; further, to suppress etching during the adsorption step, the Cl/O adsorption time was maintained shorter than 20 s/cycle as the optimized adsorption condition for the physical anisotropic ALE.) For the desorption step, 50 sccm of Ar gas was used while applying +10 to +50 V to the first grid and −100 V to the second grid for the extraction of directional Ar^+ ion beams and to desorb the chemisorbed species. For both types of ALE methods, 50 sccm of Ar gas flowed for 10 s was used for the purge steps after the adsorption for the etchant purging and after the desorption for the etch-product purging. The substrate temperature was maintained at room temperature.

3. Results and discussion

Using two Cr ALE methods, i.e. (I) the chemical anisotropic ALE method, and (II) the physical anisotropic ALE method, Cr was etched and the results are shown in figures 3 and 4, respectively. Figure 3(a) shows the etch depths of Cr, Si, SiO_2, and Si_3N_4 measured as a function of Cl^+ reactive ion beam energy (i.e. first grid voltage) while exposing 20 min to the Cl^+ ion beam only without the adsorption step (the actual Cl^+ ion beam energy distribution measured as a function of first grid voltage is shown in figure S1, available online at stacks.iop.org/NANO/30/085303/mmedia). As shown in figure 3(a), Cr was not etched until +20 V, but the Cr etch rate was increased with the increase in Cl^+ ion beam up to +70 V. For other materials, Si, Si_3N_4, and SiO_2 were not etched until +10 V, +30 V, and > +70 V, respectively, and Si indicated the highest etch rate among the materials investigated. Figure 3(b) shows the etch depths of Cr, Si, SiO_2, and Si_3N_4 measured as a function of Cl^+ reactive ion beam exposure time during the ALE desorption step without the adsorption step. For the Cl^+ ion beam energy, +10 V of the first grid voltage (9–18 eV of the Cl^+ ion energy distribution; see figure S1) was used and the etch depth was measured after the exposure for 100 cycles. As shown, no Cr etching was observed when the exposure time is shorter than 20 s/cycle. In the case of silicon, no etching was observed for the exposure time shorter than 20 s/cycle, similar to Cr, but the etch rate was faster than that of Cr when the exposure time was longer than 20 s/cycle. In the case of Si_3N_4, no etching was observed until 60 s/cycle. No etching was observed for SiO_2. From the results of figures 3(a) and (b), +10 V of the first grid voltage and 10 s/cycle of desorption time were chosen as the Cl^+ ion desorption conditions for Cr ALE. The measured etch depth by Cr ALE while varying the oxygen radical adsorption time from 0 to 30 s is shown in figure 3(c). As shown in figure 3(c), for the adsorption time longer than ∼8 s/cycle, the etch rate was saturated to ∼1.1 Å/cycle. It is believed that, for the adsorption time shorter than ∼8 s/cycle, owing to the formation of oxygen deficiencies CrO_x ($x < 2$),

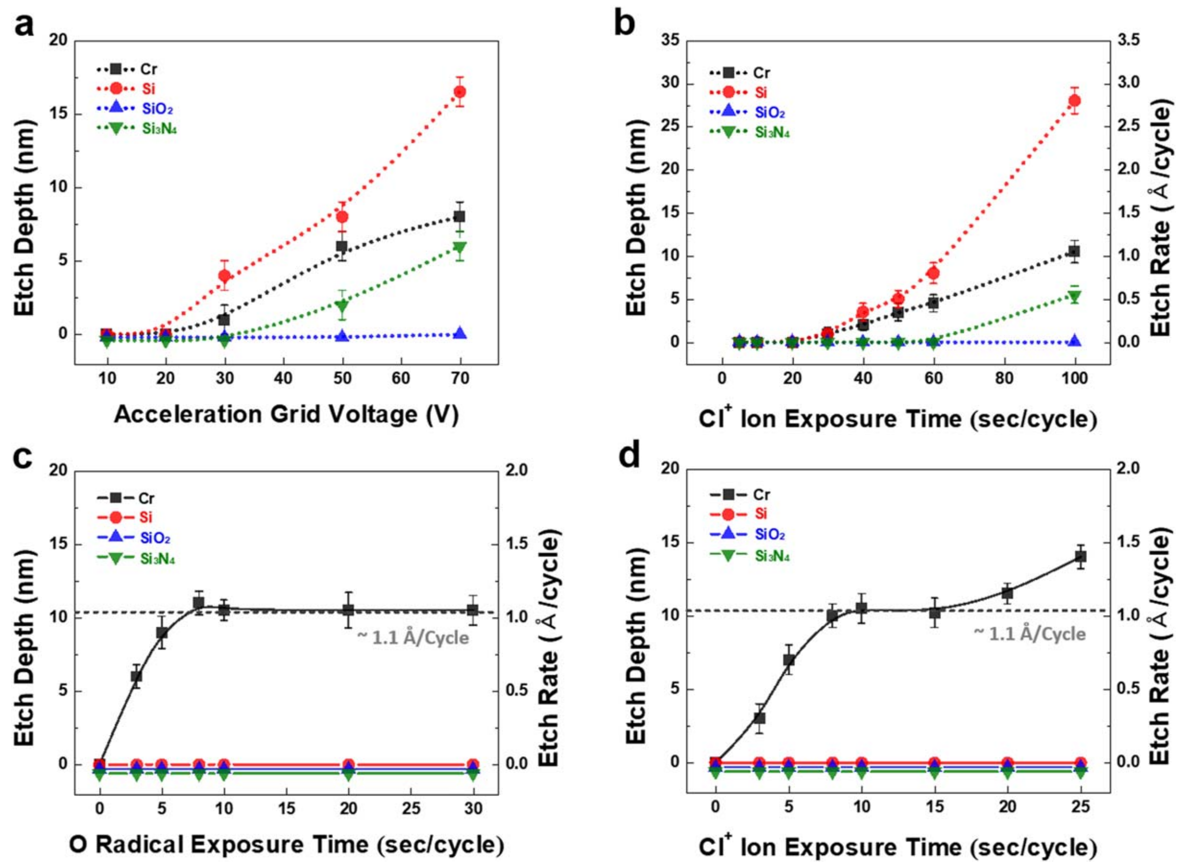

Figure 3. Cr etch depth measured as a function of (a) different first grid voltage for the Cr^+ ion exposure time of 20 min, and (b) Cl^+ ion exposure time for the first grid voltages of +10 V (Cl^+ ion energy in the range of 9–18 eV, as shown in figure S1). The Cl^+ ion etch was cyclic processed for 100 cycles without oxygen adsorption during the oxygen adsorption step. The power of the ICP ion gun for Cl^+ ion was maintained at 300 W at the process chamber pressure of 2.0 mTorr Cl_2. The second grid voltage to the ICP ion gun was maintained at −100 V for a directional ion beam while the third grid voltage was grounded. The total etch depth (Å) and etch depth/cycle (Å/cycle) of Cr, Si, SiO_2, and Si_3N_4 were measured as a function of (c) O radical exposure time (s/cycle) and (d) Cl^+ ion exposure time with the optimized ALE conditions in (a) and (b).

CrO_x was not sufficiently desorbed by Cl^+ ions by forming the less volatile CrO_xCl_y $(x < 2)$. However, when the adsorption time is longer than ∼8 s/cycle, owing to the sufficient oxidation of Cr for the stable volatile CrO_xCl_y $(x \sim 2, y \sim 2)$, a saturated etch depth/cycle is obtained. For other materials investigated such as Si, Si_3N_4, and SiO_2, no etching was observed for Cr ALE conditions possibly owing to surface oxidation even though Si and Si_3N_4 were etched with Cl^+ ion etching conditions. While maintaining the oxygen radical adsorption time at 10 s/cycle during the adsorption step, the Cl^+ ion desorption time was varied from 0 to 25 s/cycle; the measured etch depths and etch depth/cycle are shown in figure 3(d). The saturated etch depth of ∼1.1 Å/cycle was observed for the Cl^+ ion exposure time of 8–15 s/cycle. For the time less than ∼8 s/cycle, the etch rate was lower than ∼1.1 Å/cycle owing to the formation of less stoichiometric CrO_xCl_y $(x \sim 2, y < 2)$; further, for the time higher than 15 s/cycle, owing to the continuous etching of Cr by Cl^+ ions after the removal of chemisorbed CrO_xCl_y $(x \sim 2, y \sim 2)$, a layer formed on the Cr surface. (Even though no sputter etching of Cr was observed at +10 V, as shown in figure 3(a), when the Ar^+ sputter exposure time/cycle is higher than 20 s/cycle, we observed the sputter etching of Cr as shown in figures 3(b) and (d). This might be related to the measurement error and requires more investigation; however, the sputter-etched thickness of Cr etched for 100 cycles was immeasurably small when the exposure time/cycle was smaller than 20 s/cycle.) For other materials investigated such as Si, Si_3N_4, and SiO_2, no etching was observed for Cr ALE conditions. Therefore, Cr etching by the chemical anisotropic ALE is obtained by desorption of oxidized Cr as follows:

(Cr chemical anisotropic ALE by Cl^+ ion chemical desorption of CrO_2)

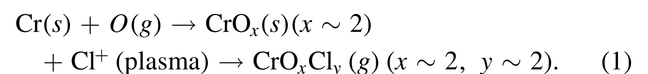

$$\mathrm{Cr}(s) + O(g) \rightarrow \mathrm{CrO}_x(s)(x \sim 2) + \mathrm{Cl}^+ \,(\text{plasma}) \rightarrow \mathrm{CrO}_x\mathrm{Cl}_y\,(g)\,(x \sim 2,\; y \sim 2). \quad (1)$$

As another method of Cr ALE, a physical anisotropic ALE method by Ar+ ion desorption after the formation of CrO_xCl_y has been investigated. Before Cr ALE, Cr and other materials such as Si, Si_3N_4, and SiO_2 were exposed to Ar^+ ions continuously with energies from 0 to +50 V (first grid voltage, the Ar^+ ion energy distribution as a function of first grid voltage is shown in figure S2) for 20 min, and their etch depths were measured. The results are shown in figure 4(a).

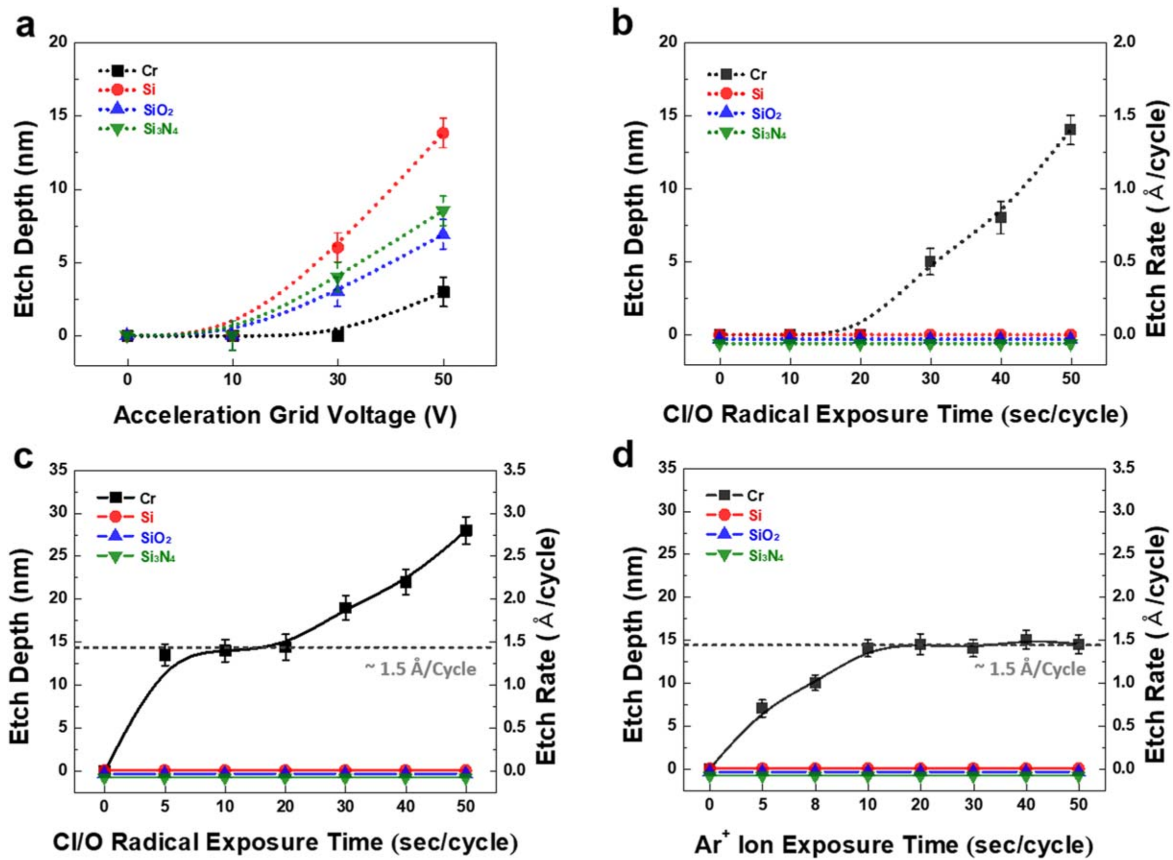

Figure 4. Cr etch depth measured as a function of (a) different first grid voltage for the Ar^+ ion exposure time of 20 min, and (b) Cl/O radical exposure time. The Cl/O radical adsorption was cyclic processed for 100 cycles of the chlorine/oxygen radical adsorption step without desorption by Ar^+ ion during the desorption step. The power of the ICP ion gun for Ar^+ ion was maintained at 300 W at the pressure of 2.0 mTorr Ar. The second grid voltage to the ICP ion gun was maintained at −100 V for a directional Ar^+ ion beam, while the third grid voltage was grounded. The etch depth (Å) and etch depth/cycle (Å/cycle) of Cr, Si, SiO_2, and Si_3N_4 measured as a function of (c) Cl/O radical exposure time (s/cycle) and (d) Ar^+ ion exposure time with the optimized ALE conditions in (a) and (b).

As shown, for Ar^+ ion exposure, Cr was not etched up to +30 V while other materials were etched for the first grid voltage higher than +10 V. It was difficult to observe the differences in the sputter threshold energies for different materials possibly owing to the smaller differences in the sputter threshold energies compared to the acceleration voltage interval, and owing to the spread of ion energy at a given acceleration voltage as shown in figure S2. Further, even though the chemical reactivity of the Cl^+ ion is higher compared to that of Ar^+ ion for the etching, the sputter etch rates by Ar^+ ions at a given acceleration voltage shown in figure 4(a) were higher than those by the Cl^+ ions in our experiment owing to the smaller Cl^+ ion flux than Ar^+ ion flux at a given acceleration voltage (i.e. at a given RF power to the ICP source, the Cl^+ ion density is lower than the Ar^+ ion density owing to the electronegativity of Cl_2). When Cr and other materials were exposed to Cl/O radicals for 100 cycles only by operating the ICP ion source with Cl_2/O_2 (1:1) without applying any grid voltage during the adsorption step and without Ar^+ ion exposure during the desorption step, as shown in figure 4(b), only Cr was etched after 10 s/cycle while other materials such as Si, Si_3N_4, and SiO_2 were not etched by Cl/O radicals possibly owing to the formation of volatile CrO_xCl_y ($x \sim 2$, $y \sim 2$) for Cr and non-volatile oxychloride formation for other silicon-based materials. From the results of figure 4(a), while maintaining the Ar^+ ion exposure condition during the desorption step at +10 V of the first grid voltage (5–9 eV of Ar^+ ion energy distribution; see figure S2) and 10 s/cycle, the Cl/O radical exposure time was varied from 0 to 50 s/cycle during the adsorption time; the results are shown in figure 4(c). As shown, for the Cl/O radical exposure time from 5 to 20 s/cycle during the adsorption step, the saturated etch rate of ∼1.5 Å/cycle was observed; meanwhile, when the exposure time is higher than 20 s/cycle, the etch depth was increased possibly owing to the spontaneous etching of Cr by Cl/O radicals, as shown in figure 4(b). The thicker etch depth per cycle of ∼1.5 Å/cycle than ∼1.1 Å/cycle for the chemical anisotropic ALE method appears to be related to the formation of the CrO_xCl_y layer that is thicker than one atomic layer on the surface. The Ar^+ ion exposure time was varied with the first grid voltage of +10 V during the desorption step while maintaining the Cl/O radical adsorption time at 10 s/cycle during the adsorption step; the measured Cr etch depth/cycle is shown in figure 4(d). As shown, owing to the desorption of all the chemisorbed CrO_xCl_y formed on the Cr surface during the adsorption step, for the Ar^+ ion exposure time higher than 10 s/cycle, a saturated Cr etch depth of ∼1.5 Å/cycle was

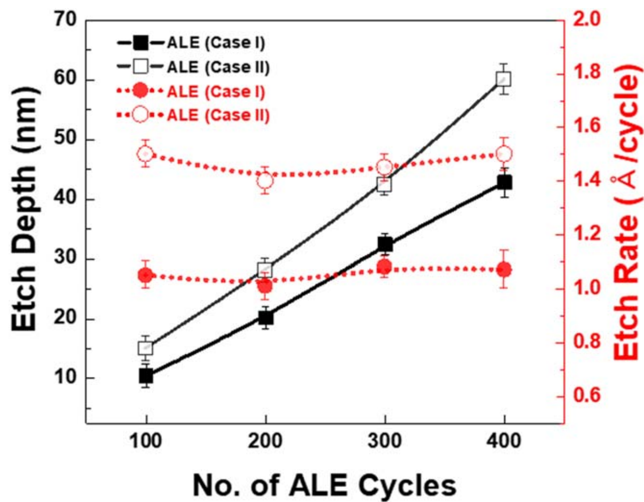

Figure 5. Etch depth (Å) and etch depth/cycle (Å/cycle) for two Cr ALE methods measured as a function of the number of ALE cycles.

obtained. It is believed that Cr ALE is obtained by the Ar^+ ion physical desorption of CrO_xCl_y ($x \sim 2$, $y \sim 2$) as follows:

(*Cr physical anisotropic ALE by Ar^+ ion desorption of CrO_xCl_y*)

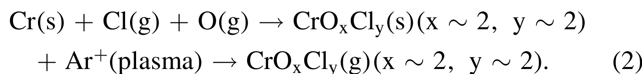

$$\mathrm{Cr(s) + Cl(g) + O(g) \rightarrow CrO_xCl_y(s)(x \sim 2,\ y \sim 2) + Ar^+(plasma) \rightarrow CrO_xCl_y(g)(x \sim 2,\ y \sim 2).} \quad (2)$$

Using the optimized Cr ALE conditions for (I) the chemical anisotropic ALE method, and (II) the physical anisotropic ALE method, the etch depth and etch rate (Å/cycle) of Cr were measured as a function of etch cycles from 100 to 400 cycles; the results are shown in figure 5. As shown, the etch depths increased linearly with increasing Cr ALE cycles for both methods; further, the etch rates remained similar at ~1.1 Å/cycle for the chemical anisotropic ALE method and at ~1.5 Å/cycle for the physical anisotropic ALE method. Therefore, the exact Cr etch depths could be controlled precisely with atomic precision by controlling the etch cycles in both ALE methods.

For the Cr ALE by the chemical anisotropic ALE method in figure 3(d) and the physical anisotropic ALE method in figure 4(d), the change in Cr surface roughness was measured as a function of Cl^+ and Ar^+ ion exposure time during the desorption step; the results are shown in figure 6. Figures 6(a)–(f) are the AFM images of the Cr surface after Cr ALE for different Cl^+ and Ar^+ ion exposure times during the desorption step; figure 6(g) shows the AFM roughness values measured as a function of Cl^+ and Ar^+ ion exposure times during the desorption step. For the AFM images, Cr ALE was performed 10 cycles. For Cr ALE by the chemical anisotropic ALE method, the oxygen exposure time was maintained at 10 s/cycle during the adsorption step and the Cl^+ ion energy was maintained at 10 V (first grid voltage) during the desorption step. For Cr ALE by the physical anisotropic ALE method, the oxygen/chlorine exposure time was maintained at 10 s/cycle during the adsorption step and the Ar^+ ion energy was maintained at 10 V (first grid voltage) during the desorption step. As shown in figure 6(g), for chemical anisotropic ALE, the surface roughness was the highest when the Cl^+ exposure time was 5 s/cycle (0.68 nm) and when the Cl^+ exposure time is increased to 10 s/cycle (0.55 nm) of the saturated etch rate condition. In physical anisotropic ALE, the surface roughness was the highest when the Ar^+ exposure time was 3 s/cycle (0.81 nm); further, when the Ar^+ exposure time is increased to 10 s/cycle (0.54 nm) of the saturated etch rate condition, the surface roughness was decreased to a value close to that of the reference (0.53 nm) for both ALE methods. It is believed that the highest surface roughness observed at 3–5 s/cycle is related to the removal of a partial CrO_x ($x \sim 2$) and CrO_xCl_y ($x \sim 2$, $y \sim 2$) layer during each etch cycle, and the low surface roughness close to that of the reference at 10 s/cycle is related to the complete removal of one surface CrO_x ($x \sim 2$) and CrO_xCl_y ($x \sim 2$, $y \sim 2$) layer during each etch cycle.

For both ALE methods, the surface binding states of Cr after ALE were investigated using XPS, and they were compared with those of the reference Cr surface and the Cr surfaces after conventional ICP-RIE using Cl_2 and Cl_2/O_2 with the etch conditions mentioned in the experimental section. The Cr ALE conditions are the same as those in figure 6. Figure 7(a) shows the narrow scan data of Cr 2*p* for the reference, Cr ALE methods, and ICP-RIE. (XPS wide scan data is shown in figure S3). As shown in the figure, in addition to Cr metal (Cr–Cr) peaks at 583.5 eV (Cr $2p_{1/2}$) and 574.2 eV (Cr $2p_{3/2}$), binding peaks related to chemically modified Cr (Cr–O, Cr–Cl–O, or Cr–Cl) at 586.4–587.6 eV (Cr $2p_{1/2}$) and 576.7–577.9 eV (Cr $2p_{3/2}$) were observed for all the samples possibly owing to the chemical surface modification of Cr during the processing and surface oxidation of Cr after exposure to air. For the Cr $2p_{3/2}$ peak, the Cr metal (Cr–Cr) peak intensities of the ALE-etched samples (ALEs I and II) were similar to that of the reference. However, for the ICP-RIE, the Cr metal (Cr–Cr) peak intensities were significantly lower and the chemically modified Cr (Cr–Cl or Cr–Cl–O) peak intensities were relatively higher than that (Cr–O) of the reference. Therefore, after ALE, a negligible chemical modification of the surface was observed while much thicker modified layers were observed on the Cr surfaces etched by ICP-RIE. Figure 7(b) shows the peak positions of the chemically modified Cr $2p_{1/2}$ and Cr $2p_{3/2}$ for reference, Cr ALE methods, and ICP-RIE. As shown in the figure, the positions of the chemically modified Cr 2*p* peaks were maintained for the ALE methods near 576.7 eV as Cr–O, similar to that of the reference (for the chemical anisotropic ALE, the peak position was slightly higher owing to the use of Cl^+ ion for the desorption step). However, for Cl_2/O_2-RIE and Cl_2-RIE, the positions of the chemically modified Cr 2*p* peaks were shifted to a higher binding energy from 576.7 eV (Cr–O) to 577.1 eV (Cr–Cl–O) and to 577.9 eV (Cr–Cl), respectively. Therefore, the XPS results indicate that the modified and damaged Cr surfaces are found after etching by ICP-RIE, while no significant damage is observed on the Cr surface after both Cr ALE methods.

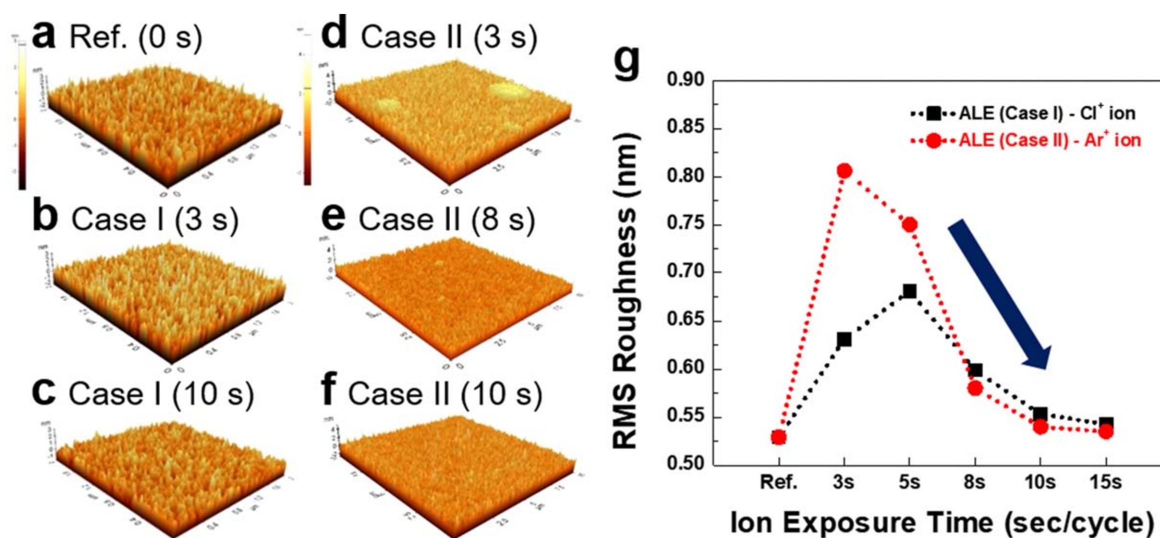

Figure 6. Surface roughness as a function of (a)–(c) Cl^+ ion exposure time during ALE for the chemical anisotropic ALE method, and (d)–(f) Ar^+ ion exposure time during ALE for the physical anisotropic ALE method investigated using AFM. The surface roughness was measured after Cr was etched for 10 cycles. For Cr ALE, the oxygen and oxygen/chlorine exposure times were maintained at 10 s/cycle during the adsorption step, and the Cl^+ and Ar^+ ion energies were maintained at 10 V (first grid voltage) during the desorption step.

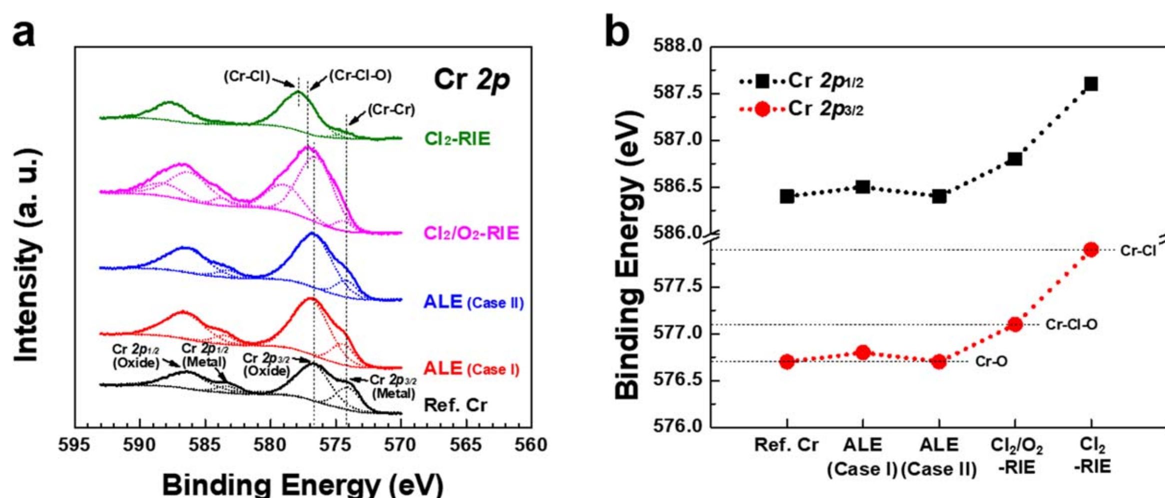

Figure 7. (a) XPS Cr 2*p* narrow scan spectra, and (b) chemically modified Cr peak positions of Cr $2p_{1/2}$ and Cr $2p_{3/2}$ for the chemical anisotropic ALE (ALE case I), the physical anisotropic ALE (ALE case II), and ICP-RIEs (Cl_2-RIE and Cl_2/O_2-RIE). As a reference, the Cr 2*p* spectrum of unetched Cr was included. For the ICP-RIE, Cr was etched for 5 min using an ICP-RIE etcher operated at 13.56 MHz, 100 W, and 13.56 MHz 50 W bias voltage, 5.0 mTorr of Cl_2 (for Cl_2-RIE), and Cl_2/O_2 (1:1) (for Cl_2/O_2-RIE). The Cr ALE conditions are the same as those in figure 6.

4. Conclusion

In this study, two different Cr ALE methods, i.e. (I) a chemical anisotropic ALE method using oxygen radicals for adsorption and Cl^+ ion for desorption ion, and (II) a physical anisotropic ALE method using oxygen/chlorine radicals for adsorption and Ar^+ ion for desorption ion, were investigated, and their etch characteristics were studied. (I) For the chemical anisotropic ALE method, the Cr ALE condition was related to the formation of stable CrO_x ($x \sim 2$) on the Cr surface during the adsorption and removal of CrO_x by forming the volatile CrO_xCl_y ($x \sim 2$, $y \sim 2$), which can be desorbed by a low-energy Cl^+ ion (+10 V of first grid voltage; 9–18 eV of Cl^+ ion energy distribution) during the desorption step. (II) For the physical anisotropic ALE method, the Cr ALE condition was related to the formation of CrO_xCl_y ($x \sim 2$, $y \sim 2$) on the surface using Cl/O radicals during the adsorption step and the removal of CrO_xCl_y using the low-energy Ar^+ ion (+10 V of first grid voltage; 5–9 eV of Ar^+ ion energy distribution) during the desorption step. When a stable CrO_xCl_y compound was formed on the Cr surface, the compound can be vaporized easily; therefore, an ALE window appeared for the Cl/O radical adsorption time of 5–20 s/cycle during the adsorption step for the physical anisotropic ALE method. In the chemical anisotropic ALE method, an ALE window also appeared for the Cl^+ ion desorption time of 8–15 s/cycle during the desorption step because of the etching of the exposed Cr surface by Cl^+ ions

after the CrO_xCl_y compound layer was desorbed. Using both ALE methods, saturated Cr etch rates of approximately 1.1 Å/cycle (chemical) and 1.5 Å/cycle (physical) could be obtained, and the etch depth/cycle remained constant regardless of the etch cycles up to 400 cycles; therefore, the Cr etch depth could be controlled with atomic precision by controlling the etch cycles in addition to the infinite etch selectivities over Si-based materials. Further, the surface roughness and chemical composition of the Cr surface were maintained before and after the ALE cycles.

Acknowledgments

This work was supported by the National Research Foundation of Korea (NRF) grant funded by the Korean government (MSIT) (2018R1A2A3074950) and the Nano Material Technology Development Program through the National Research Foundation Korea (NRF), funded by the Ministry of Education, Science, and Technology (2016M3A7B4910429).

ORCID iDs

Geun Young Yeom https://orcid.org/0000-0001-6603-2193

References

[1] George S M 2010 *Chem. Rev.* **110** 111–31
[2] Johnson R W, Hultqvist A and Bent S F 2014 *Mater. Today* **17** 5
[3] Oehrlein G S, Metzler D and Lia C 2015 *ECS J. Solid State Sci. Technol.* **4** N5041–53
[4] Kanarik K J, Lill T, Hudson E A, Sriraman S, Tan S, Marks J, Vahedi V and Gottscho. R A 2015 *J. Vac. Sci. Technol.* A **33** 2
[5] Keren J *et al* 2017 *J. Vac. Sci. Technol.* A **35** 05C302
[6] Lee Y, DuMont J W and George S M 2015 *J. Phys. Chem.* C **119** 25385–93
[7] Athavale S D and Economou D J 1996 *J. Vac. Sci. Technol.* B **14** 6
[8] Ranjan A, Wang M, Sherpa S D, Rastogi V, Koshiishi A and Ventzek. P L G 2016 *J. Vac. Sci. Technol.* A **34** 3
[9] Park J W, Kim D S, Mun M K, Lee W O, Kim K S and Yeom G Y 2017 *J. Phys. D: Appl. Phys.* **50** 254007
[10] Lim W S, Park S D, Park B J and Yeom G Y 2008 *Surf. Coat. Technol.* **202** 5701–4
[11] Kaler S S, Lou Q, Donnelly V M and Economou D J 2017 *J. Phys. D: Appl. Phys.* **50** 234001
[12] Ishii Y, Okuma K, Saldana T, Maeda K, Negishi N and Manos J 2017 *Japan. J. Appl. Phys.* **56** 06HB07
[13] Lim W S, Kim Y Y, Kim H K, Jang S J, Kwon N Y, Park B J, Ahn J-H, Chung I, Hong B H and Yeom. G Y 2012 *Carbon* **50** 429–35
[14] Xiao S, Xiao1 P, Zhang X, Yan D, Gu X, Qin F, Ni Z, Han Z J and Ostrikov K (K) 2016 *Sci. Rep.* **6** 19945
[15] Hurley R E and Gamble H S 2001 *Vacuum* **63** 627–39
[16] Buie M J, Stoehr B, Buxbaum A and Ruhl G 2002 *Proc. SPIE* **4562** 616
[17] Garetto A, Stuckey J and Butler D 2010 *Proc. SPIE* **7823** 54
[18] McIntyre G *et al* 2010 *J. Micro/Nanolith. MEMS MOEMS* **9** 013010
[19] Zhang S, Shen M, Xu Y, Wu Q, Lin Y and Gu Y 2012 *ECS Trans.* **44** 249–56
[20] Hattori S, Tamano J, Yamada M, Ieda M, Morita S, Yoneda K and Ishibashi S 1987 *Thin Solid Films* **83** 189–94
[21] Oh C, Kang M and Hahn J W 2016 *Vacuum* **123** 76–81
[22] Kang S-Y, Kwon K-H, Kim S-I, Lee S-K, Jung M-Y, Cho Y-R, Song Y-H, Lee J H and Cho K-I 2001 *J. Electrochem. Soc.* **148** G237–40
[23] Wu B 2006 *J. Vac. Sci. Technol.* B **24** 1
[24] Zau G C H and Sawin H H 1992 *J. Electrochem. Soc.* **139** 1
[25] Kwon K-H, Kang S-Y, Park S-H, Sung H-K, Kim D-K and Moon J-H 1999 *J. Mater. Sci. Lett.* **18** 1197–200